2011

Low-energy Electron Production By Relativistic Runaway Electron Avalanches In Air

Joseph R. Dwyer

Leonid P. Babich

Low-energy electron production by relativistic runaway electron avalanches in air

Joseph R. Dwyer[1] and Leonid P. Babich[2]

Received 24 January 2011; revised 31 May 2011; accepted 8 June 2011; published 7 September 2011.

[1] This paper investigates the production of low-energy (few eV) electrons by relativistic runaway electron avalanches. This work is motivated by a growing body of literature that claims that runaway electron avalanches produce an anomalous growth of low-energy electrons and hence an anomalously large electrical conductivity, a factor of 50 larger than expected from standard calculations. Such large enhancements would have a substantial impact on properties of runaway electron avalanches and their observable effects. Indeed, these purportedly large conductivities have been used to argue that runaway electron avalanches result in a novel form of electrical breakdown called "runaway breakdown." In this paper, we present simple analytical calculations, detailed Monte Carlo simulations, and a review of the experimental literature to show that no such anomalous growth of low-energy electron populations exists. Consequently, estimates of the conductivity generated by a runaway electron avalanche have been greatly exaggerated in many previous papers, drawing into question several of the claims about runaway breakdown.

Citation: Dwyer, J. R., and L. P. Babich (2011), Low-energy electron production by relativistic runaway electron avalanches in air, *J. Geophys. Res.*, *116*, A09301, doi:10.1029/2011JA016494.

1. Introduction

[2] In 1925, C. T. R. Wilson discovered the runaway electron mechanism for which electrons may obtain large energies from static electric fields in air [*Wilson*, 1925]. Specifically, when the rate of energy gain from an electric field exceeds the rate of energy loss from interactions with air then the energy of an electron will increase and it will "run away." The name "runaway electron" was introduced in 1926 by *Eddington* [1926]. In 1992, *Gurevich et al.* [1992] showed that when Møller scattering (electron-electron elastic scattering) is included, the runaway electrons described by Wilson will also undergo avalanche multiplication, resulting in a large number or relativistic runaway electrons for each energetic seed electron injected into the high-field region. Interestingly, on the basis of an analysis of research notes by C. T. R. Wilson, *Williams* [2010] argued that Wilson was aware of the runaway electron avalanche multiplication, referring to it as a "snowball effect." This avalanche mechanism is commonly referred to as the relativistic runaway electron avalanche (RREA) mechanism [*Babich et al.*, 1998, 2001]. The threshold electric field for RREA multiplication is E_{th} = 284 kV/m × n, where n is the density of air relative to that at sea level, an order of magnitude smaller than the conventional breakdown threshold field [*Dwyer*, 2003]. Because electric fields exceeding the RREA threshold field have been observed inside thunderclouds [*MacGorman and Rust*, 1998; *Marshall et al.*, 2005], there has been great interest in the RREA mechanism when studying lightning initiation [*Gurevich et al.*, 1999; *Gurevich and Zybin*, 2001; *Dwyer*, 2005, 2009, 2010], narrow bipolar events (NBE) [*Smith et al.*, 1999], terrestrial gamma ray flashes (TGFs) [*Fishman et al.*, 1994; *Lehtinen et al.*, 1999; *Dwyer and Smith*, 2005; *Dwyer* 2008; *Babich et al.*, 2008], and thundercloud electrification [*Rakov and Uman*, 2003]. In particular, it has been suggested that RREAs may produce electrical breakdown inside thunderclouds at electric field strengths far below the conventional breakdown field. The hypothesized electrical breakdown of air generated by RREAs has been named "runaway breakdown" [*Gurevich and Zybin*, 2001].

[3] Conventionally, "electrical breakdown" means a development of large numbers of electron avalanches or streamers resulting in the creation of an ionized channel with such large conductivity that the electric field in the channel will collapse. Generally, in order for a discharge to be considered an electrical breakdown, the discharge must be a self-sustained process. Conversely, if the discharge requires the support of externally supplied ionization then it is not considered an electrical breakdown. There are well known discharges supported by external sources of ionization, for instance, volumetric discharges intended to pump gas lasers. Such discharges are switched off by switching off the external sources of ionization, for instance, the beam of high-energy electrons. RREAs are exactly such a process, i.e., not an electrical breakdown, since switching off the

[1]Department of Physics and Space Sciences, Florida Institute of Technology, Melbourne, Florida, USA.
[2]Russian Federal Nuclear Center, VNIIEF, Sarov, Russia.

0148-0227/11/2011JA016494

externally supplied seed particles stops the development of the discharge. Furthermore, a RREA does not necessarily lead to the collapse of the electric field. One main reason that RREAs do not lead to an electrical breakdown is the concentration of low-energy electrons is too low.

[4] In several papers spanning the last 13 years, proponents of the runaway breakdown hypothesis have stated that the mechanism introduced by *Gurevich et al.* [1992], in addition to producing energetic runaway electrons, also results in an anomalously large increase in the low-energy (few eV) electron population, resulting in an electrical conductivity more than an order of magnitude larger than expected from calculations using standard ionization rates of energetic electrons [*Gurevich and Milikh*, 1999; *Gurevich and Zybin*, 2001; *Gurevich et al.*, 2004]. This anomalous increase in the low-energy electron population, in turn, has been used to argue that "runaway breakdown" is indeed a true electrical breakdown and to explain various atmospheric phenomena [*Milikh and Roussel-Dupré*, 2010]. Recently, Dwyer has argued that the conductivity generated by the runaway electrons produced by the RREA mechanism is too low to result in electrical breakdown [*Dwyer*, 2005, 2007, 2008].

[5] In this paper, we present results of analytical calculations, Monte Carlo simulations and a review of experimental data that all show that there is no anomalous increase in the low-energy electron populations during RREAs and that the conductivity that is produced by RREA agrees with standard ionization rates. Because the conductivity that is predicted by the theoretical work supporting runaway breakdown is more than an order of magnitude too large, we shall argue that the runaway breakdown hypothesis is not correct and that electrical breakdown directly produced by runaway electron avalanches as first proposed by *Gurevich et al.* [1992] does not occur in our atmosphere. In contrast, the RREA mechanism, along with standard ionization rates, is the correct mechanism for relativistic runaway electron production and the resulting increase in the conductivity of air. Moreover, the RREA mechanism may still be important for understanding TGFs and other atmospheric phenomena.

2. Detailed Physics of Ionization of Air by Energetic Electrons

[6] For electrons moving through air with kinetic energies above a few hundred eV most of the energy loss goes into ionizing the air, with the remainder largely going into atomic excitations. The ionization/atomic excitation energy losses per unit length along the energetic particles path are well described by the Bethe equation [*Bethe and Ashkin*, 1953]:

$$F_b(\varepsilon') \equiv -\frac{d\varepsilon'}{dx} = \frac{2\pi N_{air} Z r_e^2 mc^2}{\beta'^2} \cdot \left[\ln\left(\frac{m^2 c^4 (\gamma'^2 - 1)(\gamma' - 1)}{I^2} \right) - \left(1 + \frac{2}{\gamma'} - \frac{1}{\gamma'^2} \right) \ln 2 + \frac{1}{\gamma'^2} + \frac{(\gamma' - 1)^2}{8\gamma'^2} - \delta_{den}(\gamma') \right], \quad (1)$$

where N_{air} is the number density of the gas atoms (N_{air} = 5.39×10^{25} m^{-3} for air at sea level) and Z is the average atomic number of the gas atoms (Z = 7.26 for air), r_e = 2.818×10^{-15} m is the classical electron radius, mc^2 = 511 keV is the rest energy of an electron, $\beta' = v'/c$, $\gamma' = 1/\sqrt{1 - \beta'^2}$ is the Lorentz factor of the energetic electron, I is the effective ionization potential (e.g., I = 85.7 eV for air), and δ_{den} is a correction due to the density effect. For air, the density effect correction is very small below 30 MeV and increases only slowly above that energy. The density effect also becomes less important at higher altitudes where the density of air is lower. Equation (1) takes into account the generation of secondary electrons of all energies up to half of the primary electron's energy, the maximum possible energy. These secondary electrons will also ionize the air, also according to equation (1). The energetic secondary electrons are called "delta rays" or "knock-on electrons" and will sometimes travel considerable distances before stopping. Note that in this paper we use primed symbols to denote the incident electrons (e.g., runaway electrons) and the unprimed symbols to denote secondary electrons (e.g., delta rays).

[7] To calculate the total number of free low-energy (few eV) electrons produced by ionization, the total energy deposited in the air (from equation (1)) is divided by the W value (W = 34 eV for air) [*Jesse and Sadauskis*, 1955; *Knoll*, 2000]:

$$\alpha = F_b(\varepsilon')/W. \quad (2)$$

Equation (2) is valid for electric fields less than the conventional breakdown field. The W value is an experimentally determined quantity that gives the average deposited energy by ionizing particles or radiation required to produce one electron-ion pair in the gas [*Valentine and Curran*, 1958]. It includes the various ionization potentials plus the amount of energy that goes into excitations rather than ionization and the kinetic energy of secondary electrons. The W value is remarkably constant, applying to different types of energetic radiation (X-rays, gamma rays, energetic electrons, etc.) over a very wide range of energies and electric fields [*Weiss and Bernstein* 1957; *International Commission on Radiation Units and Measurements*, 1979].

[8] As an example, consider a 1 MeV electron moving through air at sea level. According to equation (1), such electrons lose about 215,000 eV/m. This results in α = F_b(1MeV)/W = 215,000 (eV/m)/34 eV = 6300 total low-energy electrons per meter. For comparison, F_b(1 MeV)/I = 215,000 (eV/m)/85.7 eV = 2500 m^{-1} can be interpreted as the number of first generation secondary electrons per meter, created directly by soft and hard ionizing collisions of the primary 1 MeV electron. Another way of getting this number is to use directly the total ionization cross section σ_i. Proceeding from data of *Kim et al.* [2000], one can calculate $\sigma_i \approx 9.36 \times 10^{-23}$ m^2 for 1 MeV electron in air and then the inverse of the ionization mean free path $1/\lambda_i = N_{\mathrm{mol}}\ \sigma_i \approx$ 2516 m^{-1}, where $N_{\mathrm{mol}} \approx 2.69 \times 10^{25}$ m^{-3} is the molecule number density in air (Loshmidt's number). This $1/\lambda_i$ almost coincides with the above estimate F_b(1 MeV)/I of the specific first generation of secondary electrons.

[9] The average energy of relativistic runaway electrons produced by the RREA mechanisms is about 7.3 MeV [*Babich et al.*, 2004a; *Dwyer*, 2004]. Because of the slow relativistic rise in equation (1), these electrons will generate about $\alpha = F_b(7.3\ \text{MeV})/W = 7300$ low-energy electrons per meter at sea level.

[10] The production rate of low-energy electrons by each runaway electron is given by the approximate expression

$$\eta = \alpha\ v_{re}. \tag{3}$$

The average speed of a runaway electron avalanche is $v_{re} = 0.89c$, almost independent of the field [*Coleman and Dwyer*, 2006; *Babich and Bochkov*, 2011], which means that each energetic runaway electron generates low-energy electrons at a rate of $\eta = 1.9 \times 10^{12}\ \text{s}^{-1}$.

[11] If we are interested in the number of low-energy electrons that are free at any given time then we need to include the attachment rate of these electrons. The low-energy electron attachment includes both three-body and two-body attachment at low altitudes and is dominated by two-body attachment at high altitudes. The attachment rate is a complicated function of air density, humidity and electric field. For the attachment times, we shall use the values presented by *Gurevich et al.* [2004], so that direct comparisons with that work can be made. Specifically, we shall use the attachment time $\tau_a = 2 \times 10^{-8}$ s at sea level. The attachment times appropriate for other cases also may be used in the equations below. For electric fields below the conventional breakdown field, the rate that low-energy electrons create additional low-energy electrons through ionization is generally small compared with the attachment rate and so can be ignored. The number of low-energy electrons is then described by

$$\frac{dN_{le}}{dt} = N_{re}\eta - \frac{N_{le}}{\tau_a}, \tag{4}$$

where N_{le} and N_{re} are the numbers (or by dividing by volume, the number densities) of low-energy and runaway electrons, respectively. For an exponentially growing runaway electron population, $N_{re} = N_o \exp(t/\tau_{re})$, where τ_{re} is the runaway electron avalanche e-folding time, then from equation (4) for $t \gg \tau_{re}, \tau_a$, the ratio of low-energy to runaway electrons is [*Gurevich et al.*, 2004]

$$\frac{N_{le}}{N_{re}} = \frac{\eta\tau_a}{\left(1 + \frac{\tau_a}{\tau_{re}}\right)}. \tag{5}$$

At sea level, equation (5) gives $\frac{N_{le}}{N_{re}} \approx 13{,}000$ to $38{,}000$, for electric field strengths between 3000 and 300 kV/m, respectively.

[12] The calculations presented in this paper are performed at sea level air density. However, both α and η scale proportional to the air density, so values at other altitudes may be easily calculated from the sea level values by multiplying by n, the density of air relative to that at sea level. This similarity of the results with changing air density may be violated in two ways: First, the density effect correction, δ_{den}, in equation (1) itself depends upon the air density, so the Bethe equation changes slightly with altitude. However, this effect is small and only influences the highest energy runaway electrons and not the low-energy electron production. Second, the low-energy electron attachment rate depends upon both the three-body and two-body attachment rates, which have different density dependences. As a result, calculations that specifically involve the attachment rate (e.g., N_{le}/N_{re}) will be sensitive to the air density.

[13] We note that the results presented in this section are based upon standard calculations that should be familiar to individuals working in many areas of physics such as particle physics, astrophysics, gas discharge physics, radiation physics, medical physics, gas filled detector technology, etc. They are well-accepted values based upon decades of research [*Sauli*, 1977]. Consequently, we consider them to be the standard results. In section 3 we shall discuss runaway breakdown theories, which disagree with these standard results.

3. Previous Calculations of the Low-Energy Electron Population

3.1. Runaway Breakdown Formulation A

[14] *Roussel-Dupré and Gurevich* [1996] state that the ratio of the number of low-energy electrons to the number of runaway electrons is $N_{le}/N_{re} = \varepsilon_{re}/W$, where ε_{re} is the mean energy of the runaway electrons and W is the energy expended to make an ion pair ($W = 34$ eV). Using the modern value of $\varepsilon_{re} = 7.3$ MeV gives $N_{le}/N_{re} = 210{,}000$, about a factor of 6–17 times larger than our value in section 2. Using equations (3) and (5), this ratio N_{le}/N_{re} may be converted into the ionization per unit length per runaway electron

$$\alpha_{RB} = \frac{\varepsilon_{re}}{W\tau_a v}\left(1 + \frac{\tau_a}{\tau_{re}}\right), \tag{6}$$

where we use the subscript RB to indicate that this is a result used in runaway breakdown calculations. Equation (6) will be later compared with our work (see Figure 4).

[15] Later, *Tierney et al.* [2005] and *Füllekrug et al.* [2010] stated that the production rate of low-energy electrons by each runaway electron is $\eta = \varepsilon_{re}/(W\tau_{re})$. In the same paper, *Tierney et al.* [2005] also stated that $N_{le}/N_{re} = \varepsilon_{re}/W$. From equation (5), we see that these two equations only agree for very high electric fields where $\tau_{re} \ll \tau_a$.

[16] Unfortunately, using ε_{re}/W as the ratio of low-energy electrons to runaway electrons does not make physical sense. This relationship only works if the ionizing particle completely deposits all of its energy in the gas volume (see Appendix A). For instance, such an expression is appropriate for X-rays depositing all their energy in a gas, but is not appropriate for runaway electrons moving through a gas volume. For runaway electrons moving through air, the rate that energy is deposited is given by the ionization energy loss rate (equation (1)), which is very different from the total kinetic energy of the electrons.

[17] Furthermore, using $\eta = \varepsilon_{re}/(W\tau_{re})$ as the ionization rate also does not make physical sense, again, because the rate of ionization is not sensitive to the particle's energy for minimum ionizing particles. To illustrate this, consider what happens if we set $\varepsilon_{re}/(W\tau_{re})$ equal to αv_{re} (equation (3)). This would require that $\varepsilon_{re} = F_b\lambda$, where $\lambda = \tau_{re}v_{re}$ is the runaway

electron *e*-folding avalanche length. In contrast, for a uniform electric field, the correct expression is $\varepsilon_{re} = (eE - F_d)\lambda$, where $F_d = 276$ keV/m is the average energy loss rate for the runaway electrons [*Babich et al.*, 2004a; *Dwyer* 2004, 2007]. Because $\lambda \approx 7.3$ MeV/$(eE - F_d)$ [*Dwyer*, 2003; *Coleman and Dwyer*, 2006], this results in $\varepsilon_{re} \sim 7.3$ MeV [*Dwyer*, 2004], independent of the electric field or the air density. In contrast, the expression from *Tierney et al.* [2005] and *Füllekrug et al.* [2010] varies greatly with the electric field and can be off by more than an order of magnitude in some cases.

[18] Finally, *Colman et al*. [2010] state that the ionization rate is $\eta = F_b v_{re} \varepsilon_{re}/W$. This hybrid of the standard expression and the *Roussel-Dupré and Gurevich* [1996], *Tierney et al.* [2005], and Füllekrug *et al.* [2010] expression, unfortunately, does not have the correct units (1/s), so it cannot be further evaluated.

3.2. Runaway Breakdown Formulation B

[19] Although the formulation of runaway breakdown described above in most cases over estimates the number of low-energy electrons produced by the runaway electrons, in the papers that use this formulation the authors did not claim that the large number of low-energy electrons was unique to runaway breakdown. In other words, presumably, they would have produced the same (overestimate) for any process involving high-energy particles propagating through a gas volume. In contrast, in a series of papers presenting an alternative formulation, the claim is made that not only is there a large enhancement in the number of low-energy electrons generated, but this enhancement is a unique property of and a defining feature of runaway breakdown.

[20] This claim of an anomalously large low-energy electron population in runaway breakdown was first described by *Gurevich and Milikh* [1999], who stated that the number of low-energy (few eV) electrons and hence the conductivity is a factor of $\ln^2(\varepsilon_c/\varepsilon_m)$ larger than expected from using standard ionization rates for the runaway electrons. Here ε_c is the energy that separates the intermediate-energy (they call them low-energy) electrons and the runaway electrons. They define $\varepsilon_c \sim 100$ keV. ε_m, according to that paper, is the maximum energy needed per ionization of an air molecule, $\varepsilon_m \sim 110$ eV. Their numbers result in an enhancement factor of $\ln^2(\varepsilon_c/\varepsilon_m) = 50$. Specifically, *Gurevich and Milikh* [1999, p. 461] state "Recent development in the kinetic theory of runaway breakdown shows that the electron distribution function grows appreciably in the low-energy range $\varepsilon \le 100$–200 keV. This leads to a significant increase in the ionization rate in comparison with ionization by runaway electrons only, given by a factor of $\ln^2(\varepsilon_c/\varepsilon_m)$." As a reference for this enhancement factor, they cite the work by *Gurevich and Zybin* [1998]. However, this paper does not specifically derive this result.

[21] According to *Gurevich and Milikh* [1999], the number of low-energy electrons per runaway electron per unit length becomes

$$\alpha_{RB} = \alpha \ln^2(\varepsilon_c/\varepsilon_m), \tag{7}$$

where α is the quantity calculated in section 2. Equation (7) will be later compared with our work (see Figure 4). Similarly, the equation for the number of low-energy electrons per runaway electron per second becomes $\eta \ln^2(\varepsilon_c/\varepsilon_m)$, where η is the quantities calculated in section 2.

[22] The first derivation of this enhancement factor that we have found appears in the work of *Gurevich et al.* [1999]. According to this paper, they find the ionization produced by the intermediate-energy electron population, with energies below the runaway electrons threshold, to be proportional to $\ln(\varepsilon_c/\varepsilon_m)$, where ε_c is the lower boundary energy of runaway particles, $\varepsilon_c \sim 1$ MeV, and ε_m in this case is apparently the lower boundary of an intermediate-energy population produced by the runaway electrons. In this paper they use $\varepsilon_m \sim 1$ keV. They further estimate without derivation that the number of intermediate-energy electrons is proportional to $N_{re}\ln(\varepsilon_c/\varepsilon_m)$, where N_{re} is the number of runaway electrons. Combining these gives the enhancement factor $\ln^2(\varepsilon_c/\varepsilon_m)$, which is again equal to 50. This is the same enhancement factor used by *Gurevich and Milikh* [1999], although the values of ε_m and ε_c were both different.

[23] In their review paper, *Gurevich and Zybin* [2001] present a similar result without derivation. They refer to this result as the "anomalous growth of conductivity" and present the intensity of free electrons generated by runaway breakdown as $Q_e \approx Q_o \exp(L/\lambda)\ln^2(\varepsilon_c/\varepsilon_m)$, where Q_o is the electron density generated by the background cosmic ray flux and $\exp(L/\lambda)$ gives the runaway electron avalanche multiplication factor over the length L, with λ being the runaway electron avalanche length. In that review, $\varepsilon_c = 100$ keV and ε_m is defined to be the mean air molecule ionization energy. Although they do not state what ε_m is, they imply that it is 100 eV, which then results in an enhancement factor of 50 as above [see also *Gurevich et al.*, 2002].

[24] *Gurevich et al*. [2004] dealt specifically with the low-energy "thermal" electron population produced during runaway breakdown. In this paper, they presented the ratio of the number of low-energy (thermal) electrons to the number of runaway electrons (>1 MeV) as $N_{le}/N_{re} \approx 1.5 \times 10^6\ n^{-1}$, where n is the density of air relative to that at standard conditions. In calculating this number they state that they included the $\ln^2(\varepsilon_c/\varepsilon_m)$ enhancement factor, using ε_c = 1 MeV and ε_m = 10 keV, which again gives a factor of 50. At sea level, their ratio of the number or low-energy electrons to the number of runaway electrons is 40 times larger than expected from our calculation in section 3.1 (equation (5)). This very large value of N_{le}/N_{re} was used by the authors in later work. For example, *Gurevich et al.* [2006] use $N_{le}/N_{re} = 3 \times 10^6$ in their calculation of amplification and nonlinear modification of runaway breakdown [see also *Gurevich and Zybin*, 2004, 2005].

[25] As we shall show below, there are two basic problems with the calculations discussed in this section: they greatly over estimate the number of intermediate-energy secondary electrons, and they double count the ionization, since the ionization from the intermediate-energy secondary electrons is already included in the ionization rate of the runaway electrons when doing the standard ionization calculation.

4. Monte Carlo Simulations of Runaway Electron Avalanches

[26] The use of Monte Carlo simulations to investigate runaway electrons has a long history. The Monte Carlo

simulation used in this work follows the work by *Lehtinen et al.* [1999]. Other examples are the works by *Babich et al.* [2001] and *Carlson et al.* [2007]. The Monte Carlo simulation of relativistic runaway electron avalanches used in this study has been discussed in detail in previous publications [*Dwyer*, 2003, 2004, 2005, 2007, 2008; *Coleman and Dwyer*, 2006; *Dwyer et al.*, 2009], and so it will only briefly be described here. This simulation includes, in an accurate form, all the important interactions involving runaway electrons, positrons, X-rays, and gamma rays. These interactions include energy losses through ionization and atomic excitation and Møller scattering. The simulation fully models elastic scattering using a shielded-Coulomb potential and includes bremsstrahlung production of X-rays and gamma rays and the subsequent propagation of the photons. In addition, the simulation includes positron propagation (and annihilation) and the generation of energetic seed electrons via Bhabha scattering of positrons and via Compton scattering, photoelectric absorption and pair production of energetic photons. Although magnetic fields can be included in the simulations, for thundercloud altitudes, where lightning initiation usually occurs, the effects of the geomagnetic field are small and so will be ignored in this study.

[27] When calculating the total ionization produced by an energetic particle, it is important to not double count the ionization. For example, if the number of secondary electrons is first calculated and then the ionization energy loss rate given by equation (1) is applied to all electrons, including the primary and secondary, then this will result in too large of a value, since the ionization from the secondary electrons is already included in equation (1). If it is desired to explicitly model the secondary electrons then it is necessary to reduce the ionization energy loss in equation (1) accordingly.

[28] The production of secondary electrons is described by Møller scattering (electron-electron elastic scattering). The Møller scattering cross section is given by [*Berestetskii et al.*, 1982]

$$\frac{d\sigma_{\text{Moller}}}{d\varepsilon} = \frac{2\pi r_e^2 mc^2}{\beta'^2}\left[\frac{(\gamma'-1)^2 m^2c^4}{\varepsilon^2(mc^2(\gamma'-1)-\varepsilon)^2} - \frac{(2\gamma'^2+2\gamma'-1)}{\varepsilon(mc^2(\gamma'-1)-\varepsilon)\gamma'^2} + \frac{1}{m^2c^4\gamma'^2}\right], \tag{8}$$

where ε is the kinetic energy of the scattered atomic electron and β' and γ' are the speed divided by c and Lorentz factor of the incident electron. Because electrons are indistinguishable particles, it cannot be said which of the two scattered electrons was the incident and which one was originally the atomic electron. It is standard to define the lower energy of the two scattered electrons to be the secondary electron (δ ray) and the more energetic of the two to be the incident electron. Consequently, the energy range of the secondary electron is defined to be $0 < \varepsilon < mc^2(\gamma'-1)/2$. In this paper, for integrations that involve the Møller scattering cross section (equation (8)), we shall set $d\sigma_{\text{Moller}}/d\varepsilon = 0$ whenever $\varepsilon > mc^2(\gamma'-1)/2$, rather than restricting the limits of integration. We note that results of the Møller scattering cross section, which describes hard ionizing collisions, differs slightly from more accurate calculations that include soft collisions for runaway electrons above about 1 MeV in energy [*Celestin and Pasko*, 2010]. In particular, for electric field magnitudes higher than ~2 MV/m, the minimum runaway electron energy is low enough so that softer collisions have an impact on the dynamics of the runaway avalanche. Although this effect should not alter the conclusions of this work, it has been shown to influence RREA amplification rates at these highest field values [*Celestin and Pasko*, 2010].

[29] Because the energy losses from Møller scattering are explicitly modeled in the simulation, these losses should not also be included in the ionization energy loss F_b. Following *Lehtinen et al.* [1999], this is remedied by subtracting off the quantity

$$\begin{aligned} F_{\text{Moller}} &= N_{air} Z \int_{\varepsilon_{\min}}^{mc^2(\gamma'-1)/2} \varepsilon \frac{d\sigma_{\text{Moller}}}{d\varepsilon} d\varepsilon \\ &= \frac{2\pi N_{air} Z r_e^2 mc^2}{\beta'^2}\left[\ln\left(\frac{mc^2(\gamma'-1)}{2\varepsilon_{\min}}\right) + 1 - \frac{\varepsilon_{\min}}{(mc^2(\gamma'-1)-\varepsilon_{\min})} - \left(1+\frac{2}{\gamma'}-\frac{1}{\gamma'^2}\right)\ln\left(\frac{2(mc^2(\gamma'-1)-\varepsilon_{\min})}{mc^2(\gamma'-1)}\right) + \frac{(\gamma'-1)^2}{8\,\gamma'^2} - \frac{\varepsilon_{\min}^2}{2m^2c^4\gamma'^2}\right] \end{aligned} \tag{9}$$

from the energy loss rate (equation (1)) when calculating the effective drag force (energy loss rate):

$$F_{eff} = F_b - F_{\text{Moller}}. \tag{10}$$

This is routine procedure used to simplify Monte Carlo calculations for runaway electrons, results of which are almost exactly the same as results obtained by full Monte Carlo codes simulating directly all elementary processes [*Babich et al.*, 2004a]. Note that the Bethe equation (equation (1)) includes the total inelastic electron energy losses due to excitation and ionization of atomic species [*Berestetskii et al.*, 1982]. Equation (9) accounts for the ionization interactions with large momentum transfer leading to a production of high-energy secondary electrons capable of running away. After subtracting equation (9) from the Bethe equation, as in equation (10), the remaining part includes the losses due to processes with small momentum transfer, namely, excitation and ionization producing low-energy electrons [*Babich*, 2004]. Finally, energy losses from bremsstrahlung are included in the simulation by fully modeling the individual bremsstrahlung interactions.

[30] At energies below a few keV, the Bethe equation differs slightly from measured energy loss rates. For values below a few keV, data from the *International Commission on Radiation Units and Measurements* [1984] are used instead of the Bethe equation. The results in this paper are not sensitive to whether the Bethe equation is used or whether the more accurate ionization rates are used. For example, for $E = 430$ kV/m at sea level, the simulation gives 6840 ± 30 low-energy electrons per runaway electron per meter along the runaway electron's trajectory when the more accurate tabulated data is used, compared with 6780 ± 30

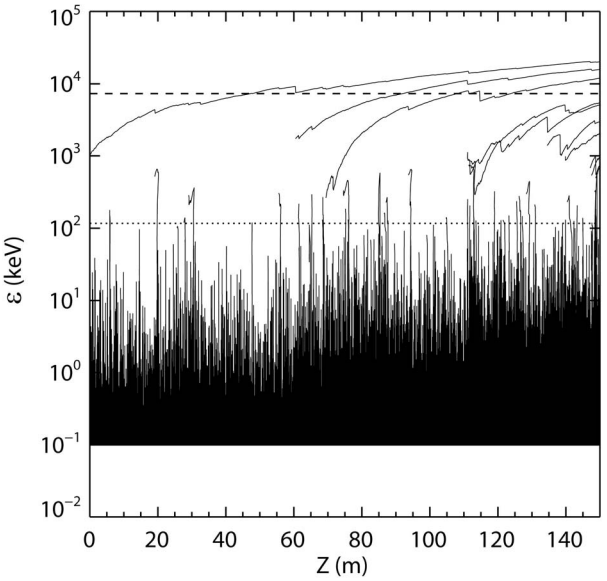

Figure 1. Example of a Monte Carlo simulation of a relativistic runaway electron avalanche in air. Each line represents the trajectory of one electron, showing the kinetic energy of the electrons versus distance. The simulation is run at 1 atm pressure and for a uniform, downward electric field of 430 kV/m ($\delta = 2$). This avalanche was initiated by injecting one 1 MeV energetic electron at the left side of the plot. The minimum energy in this simulation is $\varepsilon_{\min}$ = 100 eV. The runaway electron threshold energy, ε_{th}, is shown as a horizontal dotted line, and the average energy of the runaway electron, ε_{re}, is shown as a dashed line.

low-energy electrons when the Bethe equation is used. In this paper, we shall refer to F_b as representing the standard energy loss rate, regardless of whether equation (1) or other tabulated values are used.

[31] In the Monte Carlo simulation, all electrons (and positrons) are fully modeled for kinetic energies above the specified threshold, $\varepsilon_{\min}$. This includes new electrons and positrons created by Møller and Bhabha scattering and those created by photoelectric absorption, Compton scattering and pair production by photons. For each time step, the equations of motion of the charged particles are solved using a fourth-order Runge-Kutta method for the forces from applied electric and magnetic fields along with this effective drag force from equation (10). The energy lost to the air during each step of the electron's trajectory is found by recording the energy loss rate given by equation (10). The threshold value $\varepsilon_{\min}$ is adjustable, but is usually set to the runaway electron threshold energy,ε_{th}, which is found by setting the electric force, eE, equal to F_b in equation (1) and solving for the energy. Above this threshold, electrons may gain energy and run away. Below this threshold nearly all electrons lose energy and are eventually lost by attaching to air. As long as $\varepsilon_{\min}$ is set below the runaway electron threshold energy, ε_{th}, then the simulation will produce the same results, e.g., the same deposited energy per unit length and the same runaway electron avalanche rates, etc.. As a check, the value of $\varepsilon_{\min}$ was varied from the runaway threshold (e.g., ε_{th} ~117 keV for a 430 kV/m field) down to 100 eV and the total deposited energy was recorded. It was found that the total deposited energy did not vary by more than 5% when $\varepsilon_{\min}$ was varied over this range. For example, when $\varepsilon_{\min}$ = 117 keV, the simulation calculated 6520 ± 10 low-energy electrons per runaway electron per meter along the runaway electron's trajectory, compared with 6840 ± 30 low-energy electrons when $\varepsilon_{\min}$ = 100 eV.

[32] The secondary electrons produced by Møller scattering can themselves be energetic enough to run away and are therefore added to the simulation. In this way, the number of runaway electrons increases exponentially with time and distance for electric field strengths above the runaway avalanche threshold field, E_{th}. In addition, similar ionization rate calculations are done for positrons, but the Møller scattering equation is replaced with the Bhabha scattering equation [*Berestetskii et al.*, 1982] and the effective drag force equation is modified accordingly.

[33] Figure 1 illustrates a runaway electron avalanche produced by the Monte Carlo simulation. It shows the energy of the electrons versus position. The simulation is for about 3 avalanche lengths ($\lambda \sim 50$ m) for a uniform, downward directed electric field with a strength of 430 kV/m at sea level. This is a standard field used in several papers because $\delta = E/E_b = 2$, where E_b = 215 kV/m is the so-called breakeven field corresponding to the minimum of the Bethe energy loss curve (equation (1)). The simulation is initiated by injecting one 1 MeV electron at the left side of the plot. Other examples of runaway electron avalanches are presented by *Dwyer* [2003, 2004, 2007, 2008]. For this simulation $\varepsilon_{\min}$ = 100 eV. The runaway threshold energy, ε_{th} = 117 keV, is shown as a dotted line. As can be seen, electrons above this threshold may increase their energy and all electrons below this energy lose energy. The average energy of the runaway electrons at the end of the avalanche region is 7 MeV and is shown as a dashed line. After new electrons are created, they gain about 7 MeV over each avalanche length of 50 m. Although individual electrons can reach many tens of MeV in energy, as they increase their energy, new runaway electrons are constantly being created so that the average energy remains 7 MeV. In Figure 1, the effect of the production of energetic X-rays via bremsstrahlung and energetic secondary electrons via Møller scattering can be seen as sharp drops in the runaway electron energies.

[34] Figure 2 shows a close-up of the Monte Carlo simulation over a 10 cm distance, allowing the intermediate-energy electron trajectories to be more easily resolved. In Figure 2, runaway electrons propagate from left to right. The straggling of the electron trajectories, which is due to elastic scattering, can be seen in Figure 2. Also visible is the clumping of intermediate-energy electrons due to additional electrons being created by Møller scattering. This clumping is a well known phenomenon, seen in particle detectors.

[35] The energy deposited in the air for all electrons shown in Figure 2 are recorded by the simulation and used to calculate the ionization rate. When electron energies fall below $\varepsilon_{\min}$ = 100 eV, then their total kinetic energy is recorded at that point and those electrons are removed from the simulation. Although bremsstrahlung emission is fully modeled, for the results presented in this paper, ionization produced by the bremsstrahlung photons, which is small

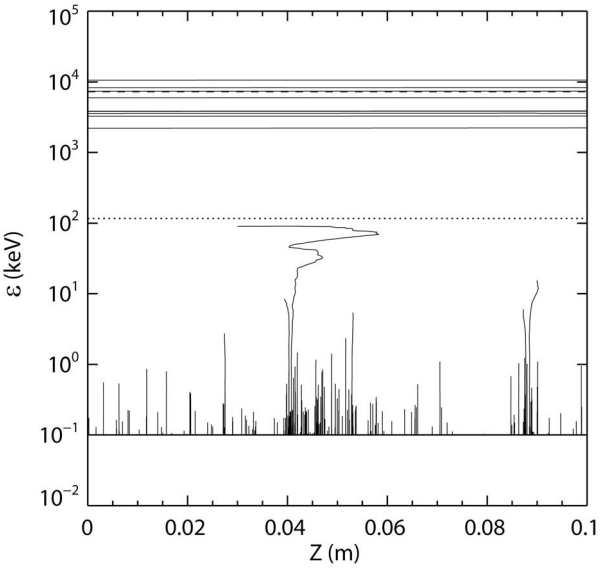

Figure 2. Example of a Monte Carlo simulation of a relativistic runaway electron avalanche in air. Each line represents the trajectory of one electron, showing the kinetic energy of the electrons versus distance. In this simulation, a close-up of the intermediate-energy electron trajectories is shown for 10 runaway electrons. The minimum energy in this simulation is $\varepsilon_{\min} = 100$ eV (solid line). The runaway electron threshold energy, ε_{th}, is shown as a horizontal dotted line, and the average energy of the runaway electron, ε_{re}, is shown as a dashed line.

compared with the ionization from the electrons, is not included in order to simplify the discussion.

5. Runaway Electron Avalanche Bookkeeping

[36] In this paper, we desire to calculate the average ionization rate produced by each runaway electron. This rate may then be used to calculate the conductivity produced by runaway electron avalanches by multiplying, for example, by the runaway electron density. Although the ionization is correctly calculated using the methods described in section 2, care must be given when calculating how much ionization is to be attributed to each runaway electron. For example, if a runaway electron produces a 100 keV secondary electron that is below the runaway threshold energy, then this secondary electron will lose its 100 keV of kinetic energy to the air, and this 100 keV will be added to the total energy lost by the runaway electron. In contrast, if the same runaway electron produces a 500 keV secondary electron that then itself runs away, this secondary electron will not deposit its 500 keV of kinetic energy in the air. Furthermore, since the secondary electron is now counted as a runaway electron, any subsequent energy loss to the air will be counted as energy loss by the new runaway electron and not the original. The proper bookkeeping of the energy loss per runaway electron is accomplished by using equation (10) instead of equation (1) when calculating the energy loss rate. This is done by integrating equation (10) over the runaway electron energy distribution function from $\varepsilon_{\min}$ to ∞. In practice, the energy $\varepsilon_{\min}$ used as the lower limit on this integration (and the integration in equation (9)) should be slightly higher than ε_{th}, since not all electrons with energies above ε_{th} will runaway. As an effective threshold energy, we define the boundary energy, ε_b, which is the energy at which there is no net flow of electrons, either gaining or losing energy. In other words, at ε_b, there are as many electrons per second losing energy as there are runaway electrons per second gaining energy. Monte Carlo simulations find that $\varepsilon_b = 870$ keV at $E = 350$ kV/m; $\varepsilon_b = 470$ keV at $E = 430$ kV/m; $\varepsilon_b = 110$ keV at $E = 1000$ kV/m; $\varepsilon_b = 45$ keV at $E = 2000$ kV/m and $\varepsilon_b = 27$ keV at $E = 3000$ kV/m. The boundary energy is a natural dividing point between the higher-energy runaway electrons and the intermediate-energy electrons.

[37] With this modification, the runaway electrons, with an exponential spectra (see section 6) of $f_{re} \propto \exp(-\varepsilon/7.3\text{ MeV})$ for $\varepsilon_b \le \varepsilon < \infty$, are found to produce $\alpha = 6770$ low-energy electrons per meter at the lowest fields ($E = 350$ kV/m) and $\alpha = 6000$ low-energy electrons per meter at the highest fields ($E = 3000$ kV/m). The small change in α with the electric field is due to the dependence of ε_b on the electric field listed above. These values are 7% to 18% lower than the value of $\alpha = 7300$ low-energy electrons per meter found in section 2, which did not take into account the creation of new runaway electrons (these results are shown in Figure 4, labeled "This work–simple model.") The ionization rate is similarly reduced according to equation (3). It is interesting that the rate that low-energy electrons are produced by runaway electron avalanches is actually slightly lower than the basic ionization rate calculated in section 2, not higher as claimed by other work outlined in section 3.

6. Simple Equation for Electrons in Air

[38] Before we present the detailed Monte Carlo calculations of runaway electron avalanches in air, it is useful to consider a very simple calculation for describing the energy spectrum (energy distribution function) of electrons in air. It can be shown that

$$\frac{df(\varepsilon,t)}{dt} = -\frac{d}{d\varepsilon}(b(\varepsilon)f(\varepsilon,t)) + N_{air}Z\int_{\varepsilon}^{\infty}\frac{d\sigma_{\text{Moller}}(\varepsilon,\varepsilon')}{d\varepsilon} \cdot v' f(\varepsilon',t)d\varepsilon', \tag{11}$$

where $b(\varepsilon) = d\varepsilon/dt$ is the average rate of change of the energy of the electrons, and $f(\varepsilon, t) = \frac{dN}{d\varepsilon}$ is the number of electrons per unit energy [*Ginzburg and Syrovatskii*, 1964]. In equation (11) and below, ε' and ε are the kinetic energies of the incident and scattered electrons, respectively. The first term on the right-hand side describes the rate of change in the number of electrons due to energy loss or gain. The second term on the right describes the creation of new electrons due to Møller scattering. Note that only incident electrons with energies above 2ε may contribute to the creation of secondary electrons at energy, ε, according to the discussion following equation (8).

[39] For an exponentially growing population with respect to time, let $f(\varepsilon, t) = f_{re}(\varepsilon)\exp(t/\tau_{re})$ for $\varepsilon > \varepsilon_b$ and $f(\varepsilon, t) = f_{\text{int}}(\varepsilon)\exp(t/\tau_{re})$ for $\varepsilon_{\min} < \varepsilon < \varepsilon_b$. Then $f_{re}(\varepsilon)$ and $f_{\text{int}}(\varepsilon)$ are the steady state runaway electron distribution function and the steady state intermediate-energy electron distribution

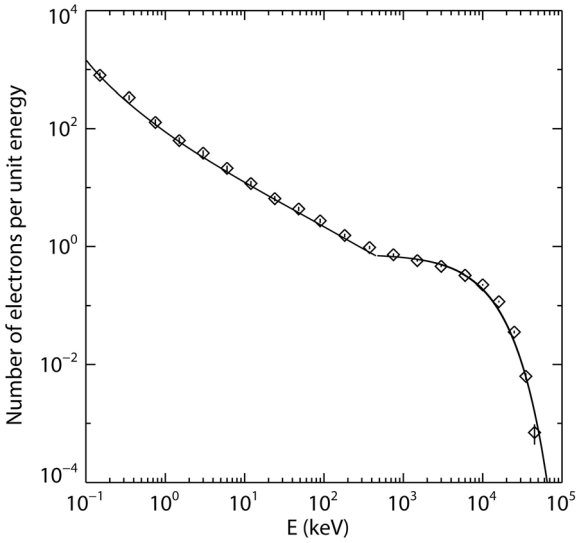

Figure 3. Number of electrons per unit energy calculated by the full Monte Carlo simulations (diamonds), along with the prediction of the simple model presented in section 6 (see equations (13), (17), and (19)).

function, respectively. We may then rewrite equation (11) as the following: For the intermediate-energy electrons,

$$\frac{f_{\text{int}}}{\tau_{re}} + \frac{d}{d\varepsilon}\left(b(\varepsilon)\, f_{\text{int}}\right) - N_{air} Z \int_{\varepsilon}^{\varepsilon_b} \frac{d\sigma_{\text{Moller}}}{d\varepsilon} v' f_{\text{int}} d\varepsilon' = N_{air} Z \int_{\varepsilon_b}^{\infty} \frac{d\sigma_{\text{Moller}}}{d\varepsilon} v' f_{re} d\varepsilon'. \tag{12}$$

The intermediate-energy electron population does not contribute to the runaway electron population. However, the runaway electron population does contribute to the intermediate-energy electron population via Møller scattering. This appears as a source term on the RHS of equation (12). In addition, the last term on the LHS is also a Møller scattering term that takes into account electrons produced by other intermediate-energy electrons.

[40] For the runaway electrons,

$$\frac{f_{re}}{\tau_{re}} = -\frac{d}{d\varepsilon}\left(b(\varepsilon)\, f_{re}\right) + N_{air} Z \int_{\varepsilon}^{\infty} \frac{d\sigma_{\text{Moller}}}{d\varepsilon} v' f_{re} d\varepsilon'. \tag{13}$$

Starting with equation (13) for the runaway electrons, for $\varepsilon \gg \varepsilon_b$, where ε_b is the runaway electron boundary energy, the electrons runaway in a direction opposite the applied electric field vector, resulting in a field-aligned beam. Therefore, $b(\varepsilon) \approx v(eE - F_b)$. For relativistic electrons, $F_b(\varepsilon) \approx F_d \equiv 276$ keV/m at sea level, and $v = v_{re}$. If we consider energies that are high enough above the threshold ($\varepsilon \gg \varepsilon_b$) such that most of the new electrons are injected below that energy, then equation (13) becomes

$$\frac{f_{re}}{\lambda} = -(eE - F_d)\frac{df_{re}}{d\varepsilon}, \tag{14}$$

where $\lambda = v_{re}\tau_{re}$. The solution to this equation is

$$f_{re} = f_o \exp\left(\frac{-\varepsilon}{(eE - F_d)\lambda}\right). \tag{15}$$

Monte Carlo simulations [*Dwyer*, 2003] show that

$$\lambda \approx \frac{7.3\ \text{MeV}}{eE - F_d}. \tag{16}$$

Substituting this in equation (15) gives

$$f_{re} = f_o \exp\left(\frac{-\varepsilon}{7.3\ \text{MeV}}\right), \tag{17}$$

independent of the electric field or the density of air.

[41] For typical electric fields of interest, $\varepsilon_b \sim 100$ keV. Inspecting equation (8), it can be seen that for energies above about 1 MeV, the Møller scattering source term contributes less than 10%, so the approximation made in equation (14) is justified.

[42] For intermediate energies, 100 eV $< \varepsilon < \varepsilon_b$, the electron distribution will be approximately isotropic because of the large elastic scattering cross section at these energies. In addition the energy loss rate becomes large compared with the electric force, eE. As a result, the average change in energy is equal to the rate given by the Bethe equation (equation (1)):

$$b(\varepsilon) \approx -v\, F_b. \tag{18}$$

Equation (12) then becomes

$$\frac{f_{\text{int}}}{\tau_{re}} - \frac{d}{d\varepsilon}\left(F_b\ v\, f_{\text{int}}\right) - N_{air} Z \int_{\varepsilon}^{\varepsilon_b} \frac{d\sigma_{\text{Moller}}}{d\varepsilon} v' f_{\text{int}} d\varepsilon' = N_{air} Z \int_{\varepsilon_b}^{\infty} \frac{d\sigma_{\text{Moller}}}{d\varepsilon} v' f_{re} d\varepsilon'. \tag{19}$$

At the boundary between the intermediate-energy and runaway electron populations, ε_b, the runaway electrons are assumed to inject intermediate-energy electrons at a rate $v(\varepsilon_b)F_b(\varepsilon_b)f_{re}(\varepsilon_b)$, which then gives the solution $f_{\text{int}}(\varepsilon_b) = f_{re}(\varepsilon_b)$ at the boundary. This choice of boundary condition mainly affects the spectrum near ε_b and does not significantly affect the spectrum at energies much less than ε_b. When performing the integrations in equation (19), the limits of integration should be handled with care so that the secondary electrons are never more than one half of the incident electron energy.

[43] For a given runaway electron spectrum, the spectrum of intermediate-energy electrons, therefore, can be found from equation (19). For example, the exponential runaway electron spectrum in equation (17) can be plugged into equation (19) and then f_{int} may be found numerically. Alternatively, in this paper, the runaway electron spectrum generated by the full Monte Carlo simulation will be used. The results of this calculation are shown in Figure 3 for the electric field $E = 430$ kV/m and $\tau_{re} = 1.8 \times 10^{-7}$ s. Additional calculations are also done in Appendix B.

7. Results of Monte Carlo Simulation

[44] Figure 3 shows the differential energy spectrum ($f = dN/d\varepsilon$) for all electrons at time $t = 5\tau_{re}$, i.e., Five avalanche

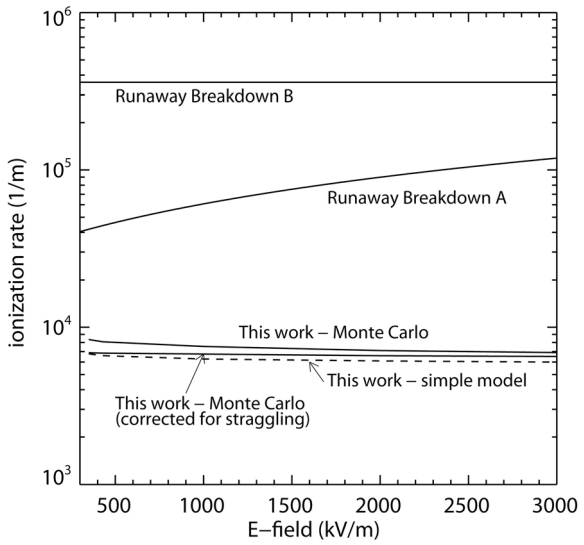

Figure 4. The ionization rate calculated by the Monte Carlo versus the electric field strength. Also shown are other runaway breakdown calculations as described in sections 3.1 and 3.2 (equations (6) and (7)). The curve labeled "This work–Monte Carlo" shows the ionization rate calculated using the full Monte Carlo simulations. The ionization rate is defined to be the number of low-energy electrons produced per runaway electron per meter along the avalanche direction. The curve labeled "This work–Monte Carlo (corrected for straggling)" is the ionization rate per runaway electron per meter traveled by the electrons. The curve labeled "This work–simple model" shows the ionization rate expected from standard calculations presented in section 5.

e-folding times, along with the solutions to the simple calculation presented in section 6 (see equations (13), (17), and (19)). For the Monte Carlo simulation, the seed electrons are injected with the exponential runaway electron spectrum above energy ε_{th}, resulting in a spectrum very close to the steady state solution. For the simulation, seed electrons are injected until the desired statistical accuracy is obtained. The simple model for the runaway electrons (equation (17)) is normalized to give the same total number of runaway electrons as the Monte Carlo. On the other hand, the curve for the intermediate-energy electrons is determined by the number of runaway electrons with no free parameters. It is found by numerically solving equation (19) for f_{int}, using the runaway electron spectrum generated by the Monte Carlo. As can be seen, the full Monte Carlo simulation, which includes all the relevant physics, agrees well with what we would expect on the basis of simple physical calculations. Although the energy spectrum of electrons does rise at lower energies, the total number of intermediate-energy electrons is actually not large (note the logarithmic energy scale).

[45] Figure 4 shows the ionization rate calculated by the Monte Carlo versus the electric field strength. The amount of deposited energy was recorded over a length of 0.05λ, at the end of a 3λ avalanche region (note as above the seed electrons are injected with the exponential runaway electron spectrum at the start of the avalanche region). In addition, the electrons are allowed to propagate an additional 1 m past the region where the deposited energy is recorded to allow any backscattered electrons to also be measured. As an example, for E = 430 kV/m (λ = 47.4 m), the runaway electron avalanche are propagated over 141 m, the ionization is recorded over a distance of 2.4 m, 1 m from the end of the avalanche region. For the simulations, seed electrons are injected until the desired statistical accuracy is obtained. Also shown are the ionization rates by other authors as discussed in sections 3.1 and 3.2. The results shown in the figure were calculated at sea level conditions. To calculate the ionization rates at other altitudes, the ionization rate and the electric fields are simply scaled with the air density. The curve labeled "This work–Monte Carlo" shows the ionization rate calculated using the full Monte Carlo simulations. This curve represents the main result of this paper. It is to be interpreted as the average number of low-energy (few eV) electrons produced per runaway electron per meter along the avalanche direction. The values of this curve are tabulated in Table 1. The curve labeled "This work–Monte Carlo (corrected for straggling)" is the ionization rate per runaway electron per meter traveled by the electrons. Because of the elastic scattering of the runaway electrons with air atoms, as the runaway electrons propagate, their trajectories will straggle (i.e., meander) slightly. This means that for every meter that the electrons move along the avalanche direction, their actual path length is slightly more than a meter because of this straggling. This results in a slightly larger ionization per meter along the avalanche direction than would occur if the runaway electrons did not scatter. The Monte Carlo simulations can measure this effect by keeping track of the total path length of all the electrons. Finally, the curve labeled "This work–simple model" shows the ionization rate expected from standard calculations presented in section 5. As can be seen, the Monte Carlo calculations that correct for straggling agree well with the simple model. In summary, the good agreement between the full Monte Carlo simulations and the expectation using standard ionization calculations illustrates that no new physics is going on with regards to the low-energy electron production, in contradiction to the various predictions for Runaway Breakdown theory.

8. Experimental Data on Ionization Rates

[46] Although the full runaway electron avalanches cannot be practically generated in laboratory experiments, nevertheless, many aspects of the runaway electron avalanche can still be studied [e.g., *Babich et al.*, 2004b]. In particular, because of the short length scales involved in ionization events, the full avalanche need not be generated in order to study the production of the low-energy electrons discussed

Table 1. Ionization per Runaway Electron per Meter Along the Avalanche Direction

Electric Field at Sea Level (kV/m)	Ionization per Meter α
350	8350 ± 60
430	8080 ± 50
1000	7540 ± 70
2000	7100 ± 60
3000	6900 ± 50

in this paper. A large amount of experimental data is available on ionization rates of energetic particles in gases including air [*Knoll*, 2000]. Since many of these experiments involved gas filled particle detectors (e.g., proportional counters, ionization chambers and drift chambers) with large electric fields, many of these experiments are directly applicable to the current discussion [*Hilke*, 2010]. As an example, ionization chamber work by collecting ions generated by energetic particles in a gas (e.g., air) gap with an electric field [*Knoll*, 2000]. Studies show that as the electric field is increased from zero, the amount of ionization measured increases because of an increase in the collection efficiency. However, for moderately strong fields, the amount of ionization collected reaches a plateau and becomes independent of the applied electric field [*Boag and Seelentag*, 1975; *Sato et al.* 1999]. This saturation is well studied and comes about when all of the ions (and electrons) produced are collected and measured [*Knoll*, 2000]. The ionization curves only start to increase again for very strong fields when low-energy electron multiplication in the gas starts occurring. Such detectors are said to enter the proportional regime. For air ionization detectors, the applied electric field can be above the runaway avalanche threshold. Because the detectors are small (usually measured in mm), the runaway electron avalanche multiplication is not important. However, anomalous growth in the ionization as described above should be apparent in such detectors if it indeed exists. To our knowledge no such anomalous growth in the ionization has been reported, despite decades of research in properties of ionization in gas field detectors.

[47] Gas filled drift chambers are another class of detectors routinely used in particle physics and cosmic ray physics, for instance [*Sauli*, 1977]. Like ionization chambers, these detectors record ionization from high-energy particles passing through gas with large electric fields. Such chambers can be several cm thick. Because these chambers are often coupled to wire proportional counters that are usually well calibrated, any anomalies in the amount of ionization produced by energetic electrons, e.g., with increasing electric fields, would certainly have been observed by now.

[48] Finally, the W value, which is the average energy required to liberate an electron-ion pair in a gas has been extensively measured for a large number of gases, under various electric fields, for many types and energies of energetic radiation and particles [*Knoll*, 2000]. It is a well established fact that the W value mainly depends upon the composition of the gas and is remarkably constant with respect to other variables such as the type of energetic radiation, etc. If an anomalous growth in the amount of ionization per energetic electron existed, then this would be recorded as a reduction in the W value. For example, if such anomalous growth were correct, experiments such as ionization chambers that measure W values for strong electric fields should measure more ionization per incident energetic particle, inferring a lower W value than 34 eV. Again to our knowledge, such variation of the W value have not been reported despite decades of in-depth measurements.

[49] We emphasize that any anomalous growth in conductivity that might be produced by runaway electron avalanches must be a local effect around each runaway electron trajectory and cannot depend upon that large scale structure of the runaway electron avalanche. As a result, such an effect should be detectable in small gas-filled detectors in the laboratory, using an energetic electron source, even though full runaway electron avalanches themselves cannot be reproduced in the laboratory because of the large voltages involved.

9. Discussion

[50] The work presented in this paper has shown that the amount of ionization produced by relativistic runaway electron avalanches is exactly what is expected using standard calculations and that no anomalous growth of the low-energy electrons occurs leading to runaway breakdown. According to several papers, the anomalous growth of the low-energy electrons is caused by the ionization from the intermediate-energy population of electrons that are above the thermal energy region but below the runaway electron threshold. In this paper, we performed detailed Monte Carlo simulations of all electrons down to 100 eV in energy, keeping track of all ionization produced by these electrons, and we find no indication of excess low-energy electron production. Because the Monte Carlo simulates every free electron down to 100 eV, it is hard to imagine how the proposed anomalous growth of low-energy electrons might occur without being captured by the detailed simulations. Because our 100 eV threshold is only a factor of 3 higher than the average energy needed to produce a free electron in air (34 eV), it is very unlikely that lowering the threshold in the calculation further would have a substantial effect. Furthermore, because 100 eV electrons only travel, at most, a few microns before losing their energy, it does not seem plausible that gas filled particle detectors would not have measured such an anomaly in the amount of ionization if produced by the electron population below 100 eV.

[51] Even for very large numbers of runaway electrons, because of lateral diffusion of the avalanche [*Dwyer*, 2010], the average distance between the runaway electrons is much larger than the atomic scale for which ionization occurs. As a result, the ionization from runaway electrons can be calculated on the basis of the ionization of individual electrons without the need to consider collective effects. It has been suggested that extensive air showers along with large amounts of runaway electron avalanche multiplication can produce nonlinear effects for which the self-generated electron and magnetic field affect the runaway electron production. However, even if such effects were true, it has not been demonstrated what impact this nonlinearity would have, if any, on the low-energy electron populations. It is also not clear if this nonlinearity can even occur in our atmosphere because of limits placed upon the electric fields by positron and X-ray feedback effects [*Dwyer*, 2003; *Babich et al.*, 2005; *Dwyer*, 2007, 2008] and from the lateral spread of the avalanches due to diffusion of the runaway electrons [*Dwyer*, 2010]. Indeed, *Dwyer* [2010] performed Monte Carlo simulations of runaway electron avalanches and showed that the lateral diffusion of the runaway electrons causes the low-energy electron density to be too low to initiate lightning, even when the avalanches are seeded by large cosmic ray extensive air showers. The results pre-

sented in this paper strengthen the conclusion of *Dwyer* [2010]. For example, using the ionization rates in this work along with the peak runaway electron fluence from *Dwyer* [2010], for a 10^{17} eV extensive air shower seeding runaway electron avalanches at 8 km altitude, the maximum low-energy electron density, N_{le}, is less than $10^7/\text{cm}^3$ for all electric field values. The electrical conductivity is then $\sigma = eN_{le}\mu_e < 2 \times 10^{-7}$ S/m, where μ_e is the electron mobility.

[52] Therefore, on the basis of this work, relativistic runaway electron avalanches appear to be exactly what this name suggests: they are avalanches of energetic electrons, analogous to the avalanches of low-energy electrons that occur at higher fields. Because low-energy avalanches alone are not synonymous with electrical breakdown, it is not clear why RREAs should be considered a form of electrical breakdown [*Roussel-Dupré et al.*, 2008]. For example, gas-filled proportional counters routinely generate large avalanches of low-energy electrons, but do not produce electrical breakdown. RREA has also been observed in the lab without an accompanying electrical breakdown [*Babich et al.* 2004b].

[53] In a recent review paper, *Milikh and Roussel-Dupré* [2010, paragraph 13] tied the term "runaway breakdown" to the large increase in the number of low-energy electrons. Specifically, they state "We note that the mechanism RB [runaway breakdown] encompasses both the avalanche of relativistic electrons and the copious production of low-energy secondary electrons that contribute significantly to the total electrical current and play an essential role in the evolution of a RB discharge." For this claim they cite *Gurevich et al.* [2004], which we discussed above. They later state that the total number of thermal electrons is 5–6 orders of magnitude higher than that of the relativistic electrons, apparently in reference to the calculation of *Gurevich et al.* [2004].

[54] The principle proponents of "runaway breakdown theory" appear to agree that a key feature of runaway breakdown is a factor of ~50 enhancement in the number of low-energy electrons over what is expected from standard calculations. This large number of low-energy electrons is repeatedly used throughout the literature to argue that RREA is in fact a form of electrical breakdown, which they call runaway breakdown, and is used to predict a range of effects that depend upon this large enhancement of low-energy electrons.

[55] The absence of this large enhancement in the low-energy electron population not only draws into question the use of the name "runaway breakdown" and the claim that it is a form of electrical breakdown [*Roussel-Dupré et al.*, 2008], it also draws into question the calculations that use this large number.

[56] It may be possible to generate more low-energy electrons by proportionally increasing the number of runaway electrons through more avalanche multiplication. However, there may be limits on how much avalanche multiplication is possible [*Dwyer*, 2003, 2007, 2008]. Increasing the amount of avalanche multiplication may also require electric potentials that are not reasonable for our atmosphere. For example, increasing the number of runaway electrons and hence the ionization by a factor of 50 would require about 4 additional runaway electron avalanche lengths. For a $\delta = 2$ field this would require an additional 90 MV of potential difference. Finally, if instead we hypothesize that the extra ionization comes from increasing the number of seed particles by increasing the energy of the cosmic ray air shower, then an air shower with roughly 50 times more energy is required. Because the flux of such high-energy air showers fall precipitously, such air showers would be almost 800 times less frequent. This would especially challenge lightning initiation and NBE models that involve air showers.

Appendix A: Derivation of Formulation A

[57] In this appendix, we derive $N_{le}/N_{re} = \varepsilon_{re}/W$ using a set of assumptions and show that these assumptions do not apply to the case of runaway electrons.

[58] Ignoring the attachment of low-energy electrons, the rate of increase of low-energy electrons is then equal to the production rate. The production rate of low-energy electrons from a distribution of runaway electrons is given by

$$\frac{dN_{le}}{dt} = \int_{\varepsilon_b}^{\infty} \frac{f_{re}(\varepsilon', t) F_b(\varepsilon') v\ (\varepsilon')}{W} d\varepsilon', \tag{A1}$$

where $f_{re}(\varepsilon, t) = \dfrac{dN_{re}}{d\varepsilon}$ is the number of runaway electrons per unit energy. If all of the runaway electrons have the same energy, ε, then $f_{re}(\varepsilon',\ t) = N_{re}\delta(\varepsilon' - \varepsilon)$. Substituting into equation (A1) gives

$$\frac{dN_{le}}{dt} = \frac{N_{re} F_b(\varepsilon) v\ (\varepsilon)}{W}, \tag{A2}$$

$$\frac{dN_{le}}{dt} = \frac{dN_{le}}{d\varepsilon}\frac{d\varepsilon}{dt} = \frac{dN_{le}}{d\varepsilon} b(\varepsilon), \tag{A3}$$

where $b(\varepsilon)$ is the average rate of change of the energy, ε, of the electrons. Therefore,

$$\frac{dN_{le}}{d\varepsilon} = \frac{N_{re} F_b(\varepsilon) v\ (\varepsilon)}{W b(\varepsilon)}. \tag{A4}$$

Integrating from the initial to final energy of the runaway electrons gives

$$\frac{N_{le}}{N_{re}} = \frac{1}{W}\int_{\varepsilon_i}^{\varepsilon_f} \frac{F_b(\varepsilon) v(\varepsilon)}{b(\varepsilon)} d\varepsilon. \tag{A5}$$

For runaway electrons moving through an electric field, $b(\varepsilon) \approx (eE - F_b(\varepsilon))v(\varepsilon)$. Also, $F_b(\varepsilon) \approx F_d$, the minimum ionizing value. This gives

$$\frac{N_{le}}{N_{re}} = \frac{F_d}{W(eE - F_d)}\int_{\varepsilon_i}^{\varepsilon_f} d\varepsilon = \frac{\Delta\varepsilon}{W}\frac{F_d}{(eE - F_d)}, \tag{A6}$$

where $\Delta\varepsilon = \varepsilon_f - \varepsilon_i$. If $eE < F_d$, then the electrons are losing energy and are no longer running away. In this case, $\varepsilon_f < \varepsilon_i$. Setting $\varepsilon_i = \varepsilon_{re}$ and $\varepsilon_f = 0$ gives

$$\frac{N_{le}}{N_{re}} = \frac{\varepsilon_{re}}{W}\frac{F_d}{(F_d - eE)}. \tag{A7}$$

As can be seen, $N_{le}/N_{re} = \varepsilon_{re}/W$ only when the electric field $E = 0$. In other words, we end up with the simple statement that the number of low-energy electrons is just the energy

deposited in the gas, when the electron loses all of its energy, divided by W.

[59] On the other hand, if $eE > F_d$, then the electrons gain energy and run away. In this case,

$$\frac{N_{le}}{N_{re}} = \frac{\varepsilon_{re}}{W}\frac{F_d}{(eE - F_d)}, \tag{A8}$$

where we used $\varepsilon_i = 0$ and $\varepsilon_f = \varepsilon_{re}$. Therefore, $N_{le}/N_{re} = \varepsilon_{re}/W$ is only true for the particular case that $eE = 2F_d$, which is not true in general. In other words, when $E \neq 0$ then $N_{le}/N_{re} = \varepsilon_{re}/W$ is no longer valid in general, even if the electron is losing energy. Furthermore, $N_{le}/N_{re} = \varepsilon_{re}/W$ can be off by an order of magnitude in cases relevant to runaway electron avalanches.

[60] Evaluating equation (A8) further, consider the fact that $\varepsilon_{re} = (eE - F_d)L$ for a uniform field, where L is the length that the electron traveled. Then,

$$\frac{N_{le}}{N_{re}} = \frac{\varepsilon_{re}}{W}\frac{F_d}{(eE - F_d)} = \frac{LF_d}{W}. \tag{A9}$$

This can be rewritten as

$$\alpha = \frac{N_{le}}{N_{re}L} = \frac{F_d}{W}, \tag{A10}$$

which is the same solution as equation (2).

Appendix B: Contribution of Intermediate-Energy Electrons

[61] In this appendix we perform a rough calculation of the low-energy electron production by intermediate-energy electrons. In contradiction to the work presented in section 3, we show that this number of the low-energy electrons is expected to be small compared with the contributions from the runaway electrons. The exact calculations from detailed Monte Carlo simulations are presented in section 7. In this appendix, we make the following simplifications for the calculation that follows. Following *Gurevich et al.* [2004], we assume that the avalanche rate, $1/\tau_{re}$, is small compared with the rate that electrons are injected into the intermediate-energy region. We assume that the number of electrons generated in the intermediate-energy region by runaway electrons is much larger than the number generated by other intermediate-energy electrons. With these two assumptions, we can drop the first and third terms on the left side of equation (19). Finally, we use the simplified version of the Møller scattering cross section

$$\frac{d\sigma_{Moller}(\varepsilon, \varepsilon')}{d\varepsilon} \approx \frac{2\pi r_e^2 mc^2}{\beta'^2 \varepsilon^2}, \quad \varepsilon \ll mc^2(\gamma' - 1), \tag{B1}$$

which is the familiar expression used to calculated delta ray production in gases [*Sauli*, 1977]. For $v_{re} \sim c$, equation (19) then becomes

$$-\frac{d}{d\varepsilon}(F_b\ vf) \approx \frac{2\pi\ r_e^2 mc^2 N_{air} Zc}{\varepsilon^2}\int_{\varepsilon_b}^{\infty} f_{re} d\varepsilon' = \frac{2\pi\ r_e^2 mc^2 N_{air} ZcN_{re}}{\varepsilon^2}, \tag{B2}$$

where $N_{re} = \int_{\varepsilon_b}^{\infty} f_{re} d\varepsilon'$ is the total number of runaway electrons integrated over all energies. Integrating both sides of equation (B2) from ε to ε_b gives the number (per unit energy) of intermediate-energy electrons at energy ε:

$$f(\varepsilon) \approx \frac{2\pi\ r_e^2 mc^2 N_{air} ZcN_{re}}{F_b(\varepsilon)v(\varepsilon)}\left(\frac{1}{\varepsilon} - \frac{1}{\varepsilon_b}\right) + f(\varepsilon_{th})\frac{F_b(\varepsilon_b)v(\varepsilon_b)}{F_b(\varepsilon)v(\varepsilon)}. \tag{B3}$$

Note that we might have chosen to integrate equation (B2) instead from ε to $\varepsilon_b/2$ according to the definition of secondary electrons creation from Møller scattering. However, little error is made with the more convenient choice of ε_b.

[62] The ionization rate caused by the intermediate-energy electrons is then

$$\begin{aligned}\eta_{\text{int}} \approx \frac{1}{W}\int_{\varepsilon_{\min}}^{\varepsilon_b} F_b vf\ d\varepsilon = &\frac{2\pi\ r_e^2 mc^2 N_{air} ZcN_{re}}{W} \\ &\cdot\left[\ln\left(\frac{\varepsilon_b}{\varepsilon_{\min}}\right) - \frac{(\varepsilon_b - \varepsilon_{\min})}{\varepsilon_b}\right] \\ &+ f(\varepsilon_b)F_b(\varepsilon_b)v(\varepsilon_b)\ (\varepsilon_b - \varepsilon_{\min})/W.\end{aligned} \tag{B4}$$

The exponential energy spectrum of the runaway electrons gives $f_{re}(\varepsilon_b) = N_{re}/7.3$ MeV. If we assume that the intermediate-energy electrons meet the runaway electrons at ε_b, i.e., $f_{\text{int}}(\varepsilon_b) = f_{re}(\varepsilon_b)$ then

$$\eta_{\text{int}} \approx \frac{2\pi\ r_e^2 mc^2 N_{air} ZcN_{re}}{W}\left[\ln\left(\frac{\varepsilon_b}{\varepsilon_{\min}}\right) - 1\right] + \frac{F_b(\varepsilon_b)v(\varepsilon_b)\varepsilon_b N_{re}}{(7.3\ \text{MeV})W}, \tag{B5}$$

where we have used $\varepsilon_{\min} \ll \varepsilon_b$.

[63] The first term on the right side of equation (B5) is at least 10 times larger than the second term for all electric field 300 kV/m $< E <$ 3000 kV/m, so the second term may be safely dropped. Therefore,

$$\eta_{\text{int}} \approx \frac{2\pi\, r_e^2 mc^2 N_{air} ZcN_{re}}{W}\left[\ln\left(\frac{\varepsilon_b}{\varepsilon_{\min}}\right) - 1\right]. \tag{B6}$$

This ionization rate can be compared with the ionization rate calculated for the runaway electrons directly:

$$\frac{\eta_{\text{int}}}{\eta_{re}} \approx \frac{\ln\left(\frac{\varepsilon_b}{\varepsilon_{\min}}\right) - 1}{\left[\ln\left(\frac{m^2c^4(\gamma^2 - 1)(\gamma - 1)}{I^2}\right) - \left(1 + \frac{2}{\gamma} - \frac{1}{\gamma^2}\right)\ln 2 + \frac{1}{\gamma^2} + \frac{(\gamma - 1)^2}{8\gamma^2} - \delta(\gamma)\right]} \approx \frac{\ln\left(\frac{\varepsilon_b}{\varepsilon_{\min}}\right)}{\ln\left(\frac{\varepsilon_{re}^3}{I^2 mc^2}\right)} \approx 0.36. \tag{B7}$$

First, as can be seen, the contribution to the ionization from the intermediate electrons is small. In contrast, the result presented in section 3 is 50, a factor of 140 too large. Second, this contribution is already taken into account when calculating ionization rate from the runaway electrons directly, $\eta = \alpha v_{re}$, so it should not be added in separately anyway.

Notation

α ionization (electron-ion pairs) per unit length per runaway electron.

$b(\varepsilon)$ average rate of change of energy per second for the electron.

$\beta = v/c$ speed of a secondary electron divided by c.

$\beta' = v'/c$ speed of an incident electron divided by c.

c speed of light, equal to 3×10^8 m/s.

$\frac{d\sigma_{\text{Moller}}}{d\varepsilon}$ differential Møller scattering cross section.

δ_{den} density effect correction in energy loss equation.

$\delta = E/E_b$ electric field relative to the breakeven electric field.

e charge of an electron, equal to 1.6×10^{-19} C.

ε' kinetic energy of an incident electron.

ε kinetic energy of a secondary electron.

ε_{re} average kinetic energy of runaway electrons, equal to 7.3 MeV.

$\varepsilon_{\min}$ minimum kinetic energy in calculation.

ε_{th} runaway electron threshold kinetic energy.

ε_b boundary energy, where the number of electrons gaining energy equals the number losing energy.

E electric field strength.

E_{th} runaway electron avalanche threshold field, equal to 276 kV/m.

E_b breakeven electric field, i.e., $E_b = \min(F_b)/e$, equal to 215 kV/m.

η ionization per second per runaway electron.

$f(\varepsilon, t) = \frac{dN}{d\varepsilon}$ electron distribution function (number of electrons/unit energy).

f_{int} electron distribution function for intermediate-energy electrons.

f_{re} electron distribution function for runaway electrons.

$F_b(\varepsilon') \equiv -\frac{d\varepsilon'}{dx}$ Bethe energy loss per unit length.

F_d average energy loss per unit length along avalanche direction for runaway electrons at sea level, equal to 270 kV/m.

F_{Moller} energy loss per unit length due to Møller scattering.

F_{eff} effective drag force (energy loss per unit length).

$\gamma = 1/\sqrt{1-\beta^2}$ Lorentz factor of a secondary electron.

$\gamma' = 1/\sqrt{1-\beta'^2}$ Lorentz factor of an incident electron.

I effective ionization potential of air, equal to 85.7 eV.

λ runaway electron avalanche (e-folding) length.

mc^2 rest energy of an electron, equal to 511 keV.

N_{air} density of air atoms at sea level, equal to 5.39×10^{25} m^{-3}.

N_{mol} density of air molecules at sea level (Loshmidt's number), equal to 2.69×10^{25} m^{-3}.

N_{le} total number (or number density) of low-energy electrons.

N_{re} total number (or number density) of runaway electrons.

n density of air relative to that at sea level.

r_e classical electron radius, equal to 2.818×10^{-15} m.

τ_a low-energy electron attachment time.

τ_{re} runaway electron avalanche (e-folding) time.

v speed of electrons.

v_{re} average speed of runaway electrons, equal to $0.89c$.

W average energy required to create an electron-ion pair in air, equal to 34 eV.

Z average atomic number of air atoms, equal to 7.26.

[64] **Acknowledgments.** Work done by Joseph R. Dwyer has been supported in part by NSF grant ATM 0607885 and by DARPA grant HR0011-10-1-0061. Work done by Leonid P. Babich has been supported in part by ISTC Project 3993-2010. The authors are grateful to the reviewers, whose comments improved the text significantly.

[65] Robert Lysak thanks the reviewers for their assistance in evaluating this manuscript.

References

Babich, L. P. (2004), Collision operator for relativistic electrons in a cold gas of atomic particles, *J. Exp. Theor. Phys.*, *98*, 707–718, doi:10.1134/1.1757671.

Babich, L. P., and E. I. Bochkov (2011), Deterministic methods for numerical simulation of high-energy runaway electron avalanches, *J. Exp. Theor. Phys.*, *112*, 494–503, doi:10.1134/S1063776111020014.

Babich, L. P., I. M. Kutsyk, E. N. Donskoy, and A. Y. Kudryavtsev (1998), New data on space and time scales of a relativistic runaway electron avalanche for thunderstorms environment: Monte Carlo calculations, *Phys. Lett. A*, *245*, 460–470, doi:10.1016/S0375-9601(98)00268-0.

Babich, L. P., et al. (2001), Comparison of relativistic runaway electron avalanche rates obtained from Monte Carlo simulations and kinetic equation solution, *IEEE Trans. Plasma Sci.*, *29*(3), 430–438, doi:10.1109/27.928940.

Babich, L. P., E. N. Donskoy, R. I. Il'kaev, I. M. Kutsyk, and R. A. Roussel-Dupré (2004a), Fundamental parameters of a relativistic runaway electron avalanche in air, *Plasma Phys. Rep.*, *30*, 616–624, doi:10.1134/1.1778437.

Babich, L. P., et al. (2004b), An experimental investigation of a relativistic runaway electron avalanche under standard conditions, *High Temp.*, *42*, 1–11, doi:10.1023/B:HITE.0000020085.61526.40.

Babich, L. P., E. N. Donskoy, I. M. Kutsyk, and R. A. Roussel-Dupré (2005), The feedback mechanism of runaway air breakdown, *Geophys. Res. Lett.*, *32*, L09809, doi:10.1029/2004GL021744.

Babich, L. P., A. Y. Kudryavtsev, M. L. Kudryavtseva, and I. M. Kutsyk (2008), Atmospheric gamma-ray and neutron flashes, *J. Exp. Theor. Phys.*, *106*, 65–76, doi:10.1134/S1063776108010056.

Berestetskii, V. B., E. M. Lifshitz, and L. P. Pitaevskii (1982), *Quantum Electrodynamics*, Pergamon, Oxford, U. K.

Bethe, H., and J. Ashkin (1953), Transport of radiation through the matter, in *Experimental Nuclear Physics*, vol. 1, edited by E. Segre, pp. 252–254, John Wiley, New York.

Boag, J. W., and W. W. Seelentag (1975), A general saturation curve for an ionization chamber filled with nitrogen at pressures up to 8 atmospheres, *Phys. Med. Biol.*, *20*, 624–626, doi:10.1088/0031-9155/20/4/009.

Carlson, B. E., N. G. Lehtinen, and U. S. Inan (2007), Constraints on terrestrial gamma ray flash production derived from satellite observations, *Geophys. Res. Lett.*, *34*, L08809, doi:10.1029/2006GL029229.

Celestin, S., and V. Pasko (2010), Soft collisions in relativistic runaway electron avalanches, *J. Phys. D Appl. Phys.*, *43*, 315206, doi:10.1088/0022-3727/43/31/315206.

Coleman, L. M., and J. R. Dwyer (2006), The propagation speed of runaway electron avalanches, *Geophys. Res. Lett.*, *33*, L11810, doi:10.1029/2006GL025863.

Colman, J. J., R. A. Roussel-Dupré, and L. Triplett (2010), Temporally self-similar electron distribution functions in atmospheric breakdown: The thermal runaway regime, *J. Geophys. Res.*, *115*, A00E16, doi:10.1029/2009JA014509.

Dwyer, J. R. (2003), A fundamental limit on electric fields in air, *Geophys. Res. Lett.*, *30*(20), 2055, doi:10.1029/2003GL017781.

Dwyer, J. R. (2004), Implications of X-ray emission from lightning, *Geophys. Res. Lett.*, *31*, L12102, doi:10.1029/2004GL019795.

Dwyer, J. R. (2005), The initiation of lightning by runaway air breakdown, *Geophys. Res. Lett.*, *32*, L20808, doi:10.1029/2005GL023975.

Dwyer, J. R. (2007), Relativistic breakdown in planetary atmospheres, *Phys. Plasmas*, *14*(4), 042901, doi:10.1063/1.2709652.

Dwyer, J. R. (2008), Source mechanisms of terrestrial gamma-ray flashes, *J. Geophys. Res.*, *113*, D10103, doi:10.1029/2007JD009248.

Dwyer, J. R. (2009), Energetic radiation and lightning, in *Lightning: Principles, Instruments and Applications*, edited by H. D. Betz, U. Schumann, and P. Laroche, pp. 331–346, Springer, New York.

Dwyer, J. R. (2010), Diffusion of relativistic runaway electrons and implications for lightning initiation, *J. Geophys. Res.*, *115*, A00E14, doi:10.1029/2009JA014504.

Dwyer, J. R., and D. M. Smith (2005), A comparison between Monte Carlo simulations of runaway breakdown and terrestrial gamma-ray flash observations, *Geophys. Res. Lett.*, *32*, L22804, doi:10.1029/2005GL023848.

Dwyer, J. R., M. A. Uman, and H. K. Rassoul (2009), The remote measurement of thunderstorm electrostatic fields, *J. Geophys. Res.*, *114*, D09208, doi:10.1029/2008JD011386.

Eddington, A. S. (1926), The source of stellar energy, *Nature*, *117*, 25–32, doi:10.1038/117025a0.

Fishman, G. J., et al. (1994), Discovery of intense gamma-ray flashes of atmospheric origin, *Science*, *264*, 1313–1316, doi:10.1126/science.264.5163.1313.

Füllekrug, M., R. Roussel-Dupré, E. M. D. Symbalisty, O. Chanrion, A. Odzimek, O. van der Velde, and T. Neubert (2010), Relativistic runaway breakdown in low-frequency radio, *J. Geophys. Res.*, *115*, A00E09, doi:10.1029/2009JA014468.

Ginzburg, V. L., and S. I. Syrovatskii (1964), *The Origin of Cosmic Rays*, Pergamon, London.

Gurevich, A. V., and G. M. Milikh (1999), Generation of X-rays due to multiple runaway breakdown inside thunderclouds, *Phys. Lett. A*, *262*, 457–463, doi:10.1016/S0375-9601(99)00695-7.

Gurevich, A. V., and K. P. Zybin (1998), Kinetic equation for high energy electrons in gases, *Phys. Lett. A*, *237*, 240–246, doi:10.1016/S0375-9601(97)00868-2.

Gurevich, A. V., and K. P. Zybin (2001), Runaway breakdown and electric discharges in thunderstorms, *Phys. Usp.*, *44*, 1119, doi:10.1070/PU2001v044n11ABEH000939.

Gurevich, A. V., and K. P. Zybin (2004), High energy cosmic ray particles and the most powerful discharges in thunderstorm atmosphere, *Phys. Lett. A*, *329*, 341–347, doi:10.1016/j.physleta.2004.06.094.

Gurevich, A. V., and K. P. Zybin (2005), Runaway breakdown and the mysteries of lightning, *Phys. Today*, *58*(5), 37–43, doi:10.1063/1.1995746.

Gurevich, A. V., G. M. Milikh, and R. Roussel-Dupré (1992), Runaway electron mechanism of air breakdown and preconditioning during a thunderstorm, *Phys. Lett. A*, *165*, 463–468, doi:10.1016/0375-9601(92)90348-P.

Gurevich, A. V., K. P. Zybin, and R. A. Roussel-Dupré (1999), Lightning initiation by simultaneous effect of runaway breakdown and cosmic ray showers, *Phys. Lett. A*, *254*, 79–87, doi:10.1016/S0375-9601(99)00091-2.

Gurevich, A. V., L. M. Duncan, Y. V. Medvedev, and K. P. Zybin (2002), Radio emission due to simultaneous effect of runaway breakdown and extensive atmospheric showers, *Phys. Lett. A*, *301*, 320–326, doi:10.1016/S0375-9601(02)00900-3.

Gurevich, A. V., Y. V. Medvedev, and K. P. Zybin (2004), Thermal electrons and electric current generated by runaway breakdown effect, *Phys. Lett. A*, *321*, 179–184, doi:10.1016/j.physleta.2003.10.062.

Gurevich, A. V., K. P. Zybin, and Y. V. Medvedev (2006), Amplification and nonlinear modification of runaway breakdown, *Phys. Lett. A*, *349*, 331–339, doi:10.1016/j.physleta.2005.09.074.

Hilke, H. J. (2010), Time projection chambers, *Rep. Prog. Phys.*, *73*, 116201, doi:10.1088/0034-4885/73/11/116201.

International Commission on Radiation Units and Measurements (1979), Average energy required to produce an ion pair, *Rep. 31*, Bethesda, Md.

International Commission on Radiation Units and Measurements (1984), Stopping powers of electrons and positrons, *Rep.37*, Bethesda, Md.

Jesse, W. P., and J. Sadauskis (1955), Ionization in pure gases and the average energy to make an ion pair for alpha and beta particles, *Phys. Rev.*, *97*, 1668–1670, doi:10.1103/PhysRev.97.1668.

Kim, Y.-K., J. P. Santos, and F. Parente (2000), Extension of the binary-encounter-dipole model to relativistic incident electrons, *Phys. Rev. A*, *62*, 052710, doi:10.1103/PhysRevA.62.052710.

Knoll, G. F. (2000), *Radiation Detection and Measurement*, 3rd ed., John Wiley, New York.

Lehtinen, N. G., T. F. Bell, and U. S. Inan (1999), Monte Carlo simulation of runaway MeV electron breakdown with application to red sprites and terrestrial gamma ray flashes, *J. Geophys. Res.*, *104*, 24,699–24,712, doi:10.1029/1999JA900335.

MacGorman, D. R., and W. D. Rust (1998), *The Electrical Nature of Storms*, Oxford Univ. Press, New York.

Marshall, T. C., et al. (2005), Observed electric fields associated with lightning initiation, *Geophys. Res. Lett.*, *32*, L03813, doi:10.1029/2004GL021802.

Milikh, G., and R. Roussel-Dupré (2010), Runaway breakdown and electrical discharges in thunderstorms, *J. Geophys. Res.*, *115*, A00E60, doi:10.1029/2009JA014818.

Rakov, V. A., and M. A. Uman (2003), *Lightning Physics and Effects*, *Cambridge Univ. Press*, Cambridge, U. K.

Roussel-Dupré, R., and A. V. Gurevich (1996), On runaway breakdown and upward propagating discharges, *J. Geophys. Res.*, *101*(A2), 2297–2311, doi:10.1029/95JA03278.

Roussel-Dupré, R., J. J. Colman, E. Symbalisty, D. Sentman, and V. P. Pasko (2008), Physical processes related to discharges in planetary atmospheres, *Space Sci. Rev.*, *137*, 51–82, doi:10.1007/s11214-008-9385-5.

Sato, K., H. Tokokowa, Y. Kohmura, T. Ishikawa, and M. Suzyuki (1999), The behavior of ionization chambers under the irradiation of high flux X-ray beam, *User Exp. Rep. 229*, SPring-8, Harima Science Park City, Japan.

Sauli, F. (1977), Principles of operation of multiwire proportional and drift chambers, *Rep. CERN 77-09*, Eur. Organ. for Nucl. Res., Geneva, Switzerland.

Smith, D. A., X. M. Shao, D. N. Holden, C. T. Rhodes, M. Brook, P. R. Krehbiel, M. Stanley, W. Rison, and R. J. Thomas (1999), A distinct class of isolated intracloud lightning discharges and their associated radio emissions, *J. Geophys. Res.*, *104*, 4189–4212, doi:10.1029/1998JD200045.

Tierney, H. E., R. A. Roussel-Dupré, E. M. D. Symbalisty, and W. H. Beasley (2005), Radio frequency emissions from a runaway electron avalanche model compared with intense, transient signals from thunderstorms, *J. Geophys. Res.*, *110*, D12109, doi:10.1029/2004JD005381.

Valentine, J. M., and S. C. Curran (1958), Average energy expenditure per ion pair in gases and gas mixtures, *Rep. Prog. Phys.*, *21*, 1–29, doi:10.1088/0034-4885/21/1/301.

Weiss, J., and W. Bernstein (1957), The current status of *W*, the energy to produce one ion pair in a gas, *Radiat. Res.*, *6*, 603–610, doi:10.2307/3570413.

Williams, E. R. (2010), The origin and context of C. T. R. Wilson's ideas on electron runaway in thunderclouds, *J. Geophys. Res.*, *115*, A00E50, doi:10.1029/2009JA014581.

Wilson, C. T. R. (1925), The acceleration of beta-particles in strong electric fields such as those of thunder-clouds, *Proc. Cambridge Philos. Soc.*, *22*, 534–538, doi:10.1017/S0305004100003236.

L. P. Babich, Russian Federal Nuclear Center, VNIIEF, Mira Ave. 37, 607188 Sarov, Russia. (babich@elph.vniief.ru)

J. R. Dwyer, Department of Physics and Space Sciences, Florida Institute of Technology, Melbourne, FL 32904, USA. (jdwyer@fit.edu)